International Journal of Science and Research (IJSR)
ISSN: 2319-7064
SJIF (2022): 7.942

Modeling and Analysis of a CSP-Biomass Hybrid Solar Power Plant for Rural Electrification in Cameroon

Kamgue Serge[1,2], Ndjiya Ngasop[1], Tetang Abraham[1,2] et Kuitche Alexis[1,2]

[1]Department of Electrical Engineering, Energy and Automation, National School of Agro-Industrial Sciences (ENSAI), University of Ngaoundere, Cameroon.

[2]Laboratory of Energy, and Applied Thermal (LETA), ENSAI/University of Ngaoundere, Cameroon.
Corresponding Author: Kamgue Serge
Email: *kamgueserge[at]gmail.com*
Tel: (+237) 6 96 85 64 82

Abstract: ***This study presents a comprehensive modeling and thermodynamic analysis of a concentrated solar power (CSP) plant combined with a biomass gas power plant, aimed at addressing rural electrification challenges in Northern Cameroon. Utilizing System Advisor Model (SAM) software, the solar power plants performance under varying solar irradiation conditions throughout the year was simulated. The study reveals that the electrical power output peaks at approximately 5 MWel in December and January and drops to around 1 MWel in August. The findings underscore the potential of CSP-biomass hybrid technology in enhancing rural electrification, emphasizing the importance of hybridization for consistent power supply and the role of thermal storage in extending operational hours.***

Keywords: Modelling, Simulation, Power plant, solar energy, Biomass, Hybrid

Nomenclature
CCP: Parabolic cylindrical collector
C_f: specific heat of the fluid
C_{Pf}: specific heat of fumes
h_i: enthalpy at point i
h_{is}: isentropic enthalpy at point i
L: total length of CCP
$\dot{m}_a$: air mass flow
$\dot{m}_f$: fumes mass flow
$\dot{m}_g$: gas mass flow
$\dot{m}_l$: fluid mass flow
P_i: absolute pressure at point i
PCI: Lower Calorific Value
P_{el}: electric power
ΔPcc: Pressure variation in the combustion chamber
Q_{abs}: heat flow absorbed in the CCP
Q_{ev}: steam inlet heat flow
Q_{ri}: heat flow recovered at point i
T_i: Temperature at point i
T_{el}: Liquid inlet temperature
T_{ev}: steam inlet temperature
T_{sl}: Liquid outlet temperature
T_{sv}: steam outlet temperature
$\dot{W}$: Work produced by the steam turbine
W_{TG}: Work produced by the gas turbine
η_{cc} : combustion efficiency
η_{sc} : isentropic compressor efficiency
η_{st} : isentropic turbine efficiency

1. Introduction

Access to electricity is a major challenge for countries around the world and a determining factor in human and economic development. In recent years, several nations around the world have been experiencing an energy crisis, mainly those in Africa including Cameroon. Global consumption of electrical energy has increased considerably. This is due to demographic change, the development of new technologies and the growth of emerging countries. [1].

In its National Development Strategy 2030 (SND30), the State of Cameroon has the objective in the energy industry sector of producing energy in abundant quantities to satisfy industrialization and become an exporting country of energy. For this, three orientations are retained, namely: developing the significant national hydroelectric potential; develop alternative energies to better meet specific needs; strengthen and optimize the use of biomass [2].

CSP-biomass hybrid mini-power plants are a well-accepted option not only for developing alternative sources of energy production, strengthening and optimizing the use of biomass, but also for effectively responding to the problem of rural electrification. In localities very far from the public electricity distribution network. The first reference plant in Spain proves the concept and should allow additional installation in locations with high direct normal radiation (DNI) where biomass is also available, such as the far north of Cameroon [3].

Several researchers have worked on modelling CSP/Biomass hybrid power plants. All these studies have modelled and simulated CSP/Biomass hybrid power plants in a Western environment and for the use of forest biomass as fuel in most cases, without taking into account the specificities of tropical zones in general, and those with high agro pastoral potential like the far North Cameroon. In the Sahelian zones, in addition to the problem of access to electricity, there is also that of deforestation due to the cutting of shrubs for cooking. In addition, these areas are known to be areas with high potential for cattle breeding and even agriculture. Biomass converted into biogas could therefore be an opportunity for the combined production of electricity and domestic gas. The question that emerges from this observation is the following:

is CSP/Biomass solar hybridization be applicable to respond to challenges of rural electrification in the northern zone of Cameroon?

2. Materials and Methods

2.1 Materials

To carry out this study, we will use:

- A DELL E5440 brand laptop, Inetl® Atom™ CPU N455 @1.66GHz 1.67 GHz processor; 1GB RAM.
- SAM modelling and simulation software;
- The climatic and solar databases of the Adamawa Region;
- The diagram of the study system.

The climatic characteristics of the city of Ngaoundere, capital of the Adamawa Region are given in table 1 below:

Table 1: Climatic characteristics of the city of Ngaoundere [4]

The irradiance variation in the city of Ngaoundere is given in table 2 below:

Table 2: Variation of solar irradiance in the city of Ngaoundere [5]

Month	Direct Normal Irradiance - DNI (W/m2)	Diffuse Irradiance - DHI (W/m2)	Global Irradiance - GHI (W/m2)
JAN	258	85	259
FEB	182	113	247
MAR	194	117	263
APR	124	116	218
MAY	117	104	196
JUNE	103	107	186
JULY	78	95	156
AUG	67	120	171
SEPT	88	119	184
OCT	79	106	165
NOV	255	76	250
DEC	330	56	267

The diagram of the mini mixed solar/biomass power plant to be studied is as follows:

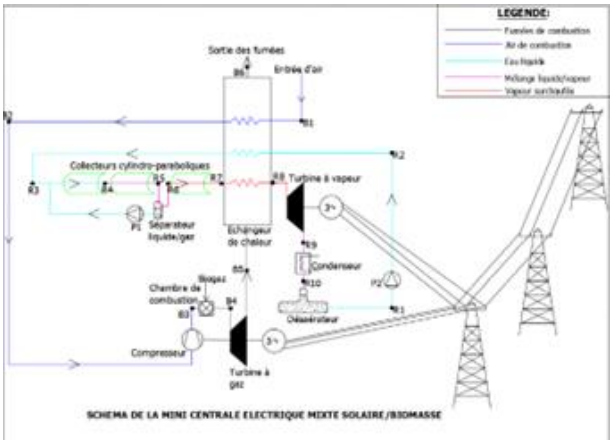

Figure 1: Diagram of the system studied

2.2 Methods

2.2.1 Thermodynamic analysis of the system

2.2.1.1 Energy analysis of the steam cycle

The energy analysis will be carried out at the level of the different components of the system.

a) Solar field

The heat exchanges at the level of the absorber tube can be modelled by the following figure:

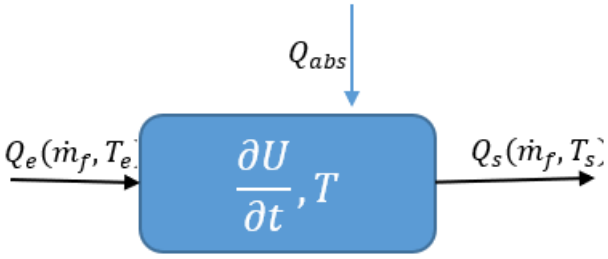

Figure 2: Model of heat exchanges at the CCP level

The heat balance in the control volume is written:

$$Q_e + Q_{abs} = \frac{\partial U}{\partial t} + Q_s \quad (1)$$

$$\frac{\partial U}{\partial t} = (mc_f + (mc)_{eq,csa}L)\frac{\partial T}{\partial t} \quad (2)$$

with m = mass of the fluid contained in the node;
L= length of CCP;
Cf = specific heat of the fluid;
$(mc)_{eq,csa}$= thermal inertia, takes into account the thermal mass of the piping, joints, insulation and other components of the CCP that cycle thermodynamically with the CCP.

$$Q_e - Q_s = \dot{m}_l c_l (T_e - T_s) = 2\dot{m}_l c_l (T_e - T) \quad (3)$$

T is the average temperature.

By replacing in the heat balance equation, we have:
$\frac{\partial T}{\partial t} = \frac{2\dot{m}_l c_l (T_e - T) + Q_{abs}}{m_l c_l + (mc)_{eq,csa}L}$, a first order differential equation. The general solution is:

$$T(t) = \frac{Q_{abs}}{2\dot{m}_l c_l} + C_1 \exp\left(\frac{2\dot{m}_l c_l}{m_l c_l + (mc)_{eq,csa}L} t\right) + T_e \quad (4)$$

$$T(t) = \frac{Q_{abs}}{2\dot{m}_l c_l} + (T_0 - T_e - \frac{Q_{abs}}{2\dot{m}_l c_l}) \exp\left(\frac{2\dot{m}_l c_l}{m_l c_l + (mc)_{eq,csa}L} t\right) + T_e \quad (5)$$

If we have N collectors, the temperature at the outlet of collector i is written:
For i=1, N

$$T_{s,i} = 2T_i - T_{e,i} = \frac{Q_{abs,i}}{\dot{m}_l c_{l,i}} + 2(T_{0,i} - T_{e,i} - \frac{Q_{abs,i}}{2\dot{m}_l c_l}) \exp\left(\frac{2\dot{m}_l c_l}{m_{l,i} c_l + (mc)_{eq,csa} L} t\right) + T_{e,i} \quad (6)$$

For i=1, N

$m_{f,i} = \rho_{f,i} L_i A_{cs,i}$

b) Fumes heat recovery

This is a recovery boiler.

A recovery boiler is an assembly of three heat exchangers placed perpendicularly and connected in series: an economizer, an evaporator associated with a tank (drum) and a super heater [6].

The heat exchange configuration in the boiler is shown in Figure 3:

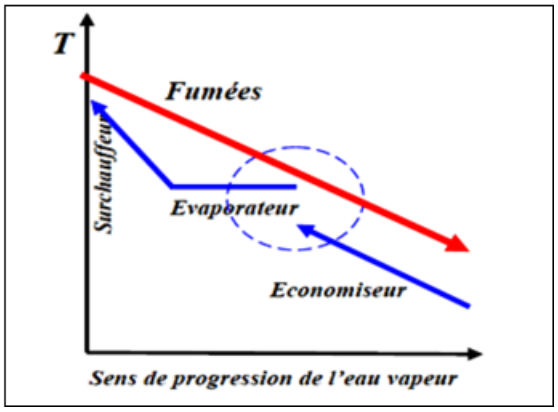

Figure 3: Configuration of a recovery boiler [6]

The heat exchanges at the level of the smoke heat recovery can be modelled in Figure 4:

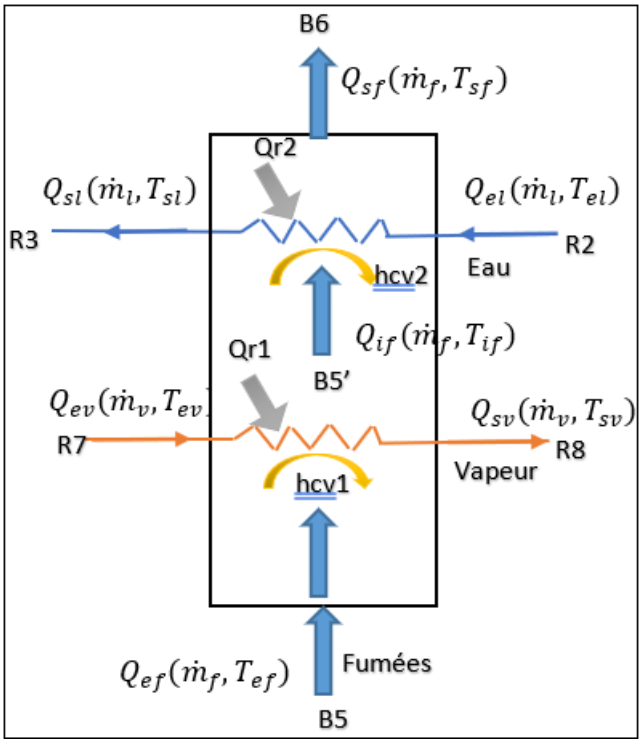

Figure 4: Model of heat exchanges at the recovery boiler

The heat balance at the super heater is written as:

$$Q_{ev} + Q_{r1} = \frac{\partial U}{\partial t} + Q_{sv} \quad (7)$$

with

$Q_{r1} = Q_{ef} - Q_{if} = \dot{m}_f c_f (T_{ef} - T_{if})$

and $Q_{ev} - Q_{sv} = \dot{m}_v c_v (T_{ev} - T_{sv})$

We pose $T = \frac{T_e + T_s}{2}$ the average steam temperature in the super heater.

$Q_{ev} - Q_{sv} = 2\dot{m}_v c_v (T_{ev} - T)$, $\frac{\partial U}{\partial t} = m_v c_v \frac{\partial T}{\partial t}$

(Thermal inertia is neglected here)

By replacing in the heat balance equation, we have:

$\frac{\partial T}{\partial t} = \frac{2\dot{m}_v c_v (T_{ev} - T) + Q_{r1}}{m_v c_v}$: First order differential equation.

The general solution to this equation is:

$$T(t) = \frac{Q_{r1}}{2\dot{m}_v c_v} + C_2 \exp\left(\frac{2\dot{m}_v}{m_v} t\right) + T_{ev} \quad (8)$$

A t=0, T=T_{02}

$T_{02} = T(0) = \frac{Q_{r1}}{2\dot{m}_v c_v} + C_2 \exp(0) + T_{ev} \rightarrow C_2 = T_{02} - T_{ev} - \frac{Q_{r1}}{2\dot{m}_v c_v}$

$$then\ T(t) = \frac{Q_{r1}}{2\dot{m}_v c_v} + (T_{02} - T_{ev} - \frac{Q_{r1}}{2\dot{m}_v c_v}) \exp\left(\frac{2\dot{m}_v}{m_v} t\right) + T_{ev}$$

$$T_{sv}(t) = \frac{Q_{r1}}{\dot{m}_v c_v} + 2(T_{02} - T_{ev} - \frac{Q_{r1}}{2\dot{m}_v c_v}) \exp\left(\frac{2\dot{m}_v}{m_v} t\right) + T_{ev} \quad (9)$$

By analogy, we have the expression for the temperature at the economizer outlet :

$$T_{sl}(t) = \frac{Q_{r2}}{\dot{m}_l c_l} + 2(T_{03} - T_{el} - \frac{Q_{r2}}{2\dot{m}_l c_l}) \exp\left(\frac{2\dot{m}_l}{m_l} t\right) + T_{el} \quad (10)$$

c) Steam turbine

At the steam turbine, an isentropic expansion of the superheated, high-pressure steam occurs. Potential energy is transformed into mechanical energy.

The heat exchange model at the steam turbine is as follows:

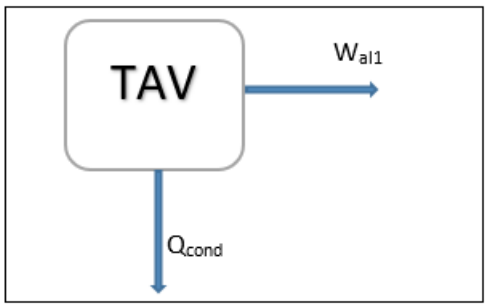

Figure 5: Model of exchanges at the steam turbine level

W_{al1}: work produced by the steam turbine and transmitted to the alternator

Q_{cond}: heat rejected to the condenser

The work produced by the steam turbine is:

$$W_{TV} = \dot{m}_v \eta_{tv} (h_8 - h_9) \quad (11)$$

The electrical power actually produced by the alternator is expressed:

$$P_{el1} = \eta_{al} W_{TV} = \dot{m}_v \eta_{al} \eta_{tv} (h_8 - h_9) \quad (12)$$

Condenser
The thermal power evacuated by the condenser is expressed:

$$Q_{cond} = \dot{m}_v(h_9 - h_1) \quad (13)$$

d) Pompe
The work provided by the pump to the fluid is expressed:

$$W_p = \frac{\dot{m}_l(h_2 - h_1)}{\eta_p} \quad (14)$$

2.2.2 Energy analysis of the gas cycle
The energy analysis will also be carried out at the level of each component of the gas cycle.

a) Compressor
The energy performance of the compressor concerns the calculation of the power necessary to compress a certain mass flow of air at a given pressure ratio, and to determine the thermodynamic values of the compressed air at the outlet [7].

The compressor is studied according to the following hypotheses:
- No heat exchange between the compressor and the environment.
- Variations in kinetic and potential energies are negligible.
- Air filter dissipation is characterized by a pressure loss factor.
- Internal irreversibility is characterized by isentropic yield.

The pressure at the compressor inlet is slightly lower than the ambient pressure due to losses in the filtration system, these losses are characterized by the pressure loss factor.

Compression is considered adiabatic but not isentropic [8], therefore characterized by an isentropic efficiency η_{sc}. Therefore, the enthalpy h_2 at the compressor outlet can be calculated from the input enthalpy h_1 and the isentropic enthalpy h_{2s} as follows:

$$h_2 = h_1 + \frac{h_{2s} - h_1}{\eta_{sc}} \quad (15)$$

The mechanical power used by the compressor can then be expressed:

$$\dot{W}_c = \frac{\dot{m}_a(h_2 - h_1)}{\eta_{méca}} \quad (16)$$

$\dot{m}_a$: compressed air flow;
$\eta_{méca}$: mechanical efficiency of the transformer.

b) Combustion chamber
The objective of steady-state combustion chamber analysis is to calculate the nominal mass flow rate of fuel required in order to operate the gas turbine [9].

The following assumptions were used for the combustion chamber model:
- Combustion is considered complete.
- Thermal losses in the combustion chamber are negligible.

In the combustion chamber a mass flow of fuel $\dot{m}_g$ (bio methane) is injected and burned with pressurized air, figure 6.

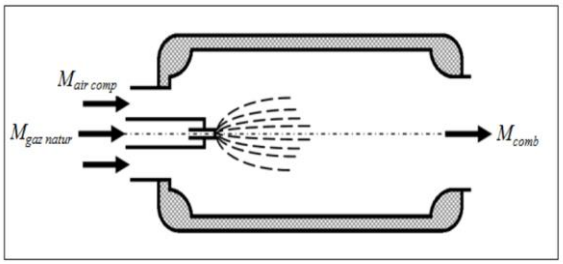

Figure 6: Combustion chamber configuration

$$C_nH_m + A\left(\frac{n+m}{4}\right).[O_2 + 3.76\,N_2] \rightarrow (n)CO_2 + \left(\frac{m}{2}\right)H_2O + \left[(A-1)\left(n+\frac{m}{4}\right)\right]O_2 + \left[3.76A\left(\frac{n+m}{4}\right)\right]N_2 \quad (17)$$

Combustion chamber output properties vary depending on air mass flow rate, fuel lower calorific value (LCV), and combustion efficiency η_{cc}

$$\dot{m}_a h_3 + \dot{m}_g PCI = \dot{m}_f h_4 + (1 - \eta_{cc})\dot{m}_g PCI \quad (18)$$

The outlet pressure of the combustion chamber (considering a pressure drop ΔPcc) is as follows:

$$\frac{P_4}{P_3} = (1 - \Delta P_{cc}) \quad (19)$$

The total mass flow rate of the combustion chamber exit gases is the sum of the compressed air and fuel flow rates:

$$\dot{m}_f = \dot{m}_a + \dot{m}_g \quad (20)$$

c) Cooling air
A mass flow fraction is extracted from the compressor, to be used for purging and sealing the gas turbine. Additionally, if the combustion chamber outlet temperature is higher than the turbine's material limits, additional air is required for cooling of the turbine blades.

The air mass flow required for gas turbine purge is relatively constant and can be considered at approximately 3% of the compressor inlet mass flow [9].

d) Gas turbine
The expansion in the turbine produces the mechanical power necessary to drive the compressor and start the electric generator. The following assumptions were used for the turbine model [8]:
- Blade cooling effects can be taken into consideration by using a fully mixed temperature at the impeller inlet.
- No heat exchange between the turbine and the environment.
- Variations in kinetic and potential energies are negligible.
- Exhaust dissipation characterized by a pressure loss factor.
- Internal dissipation characterized by an isentropic efficiency.

The power produced by the turbine is given by:

$$\dot{W}_{TG} = \dot{m}_f C_{pf}(T_4 - T_5) \quad (21)$$

$$C_{pf}(T) = 0{,}991 + \left(\frac{6{,}997T}{10^5}\right) + \left(\frac{2{,}712T^2}{10^7}\right) - \left(\frac{1{,}224T^3}{10^5}\right) \quad (22)$$

$$T_5 = T_4\left(1 - \eta_T\left(1 - \left(\frac{P_4}{P_5}\right)^{\frac{1-\gamma_g}{\gamma_g}}\right)\right) \quad (23)$$

The useful power available to the electric generator is expressed:

$$\dot{W} = \left(\eta_{is,t}\dot{W}_{TG}\right) - \left(\eta_{is,c}\dot{W}_c\right) \quad (24)$$

The electrical power produced by the alternator coupled to the gas turbine is written as:

$$P_{el2} = \eta_{al}.\dot{W} = \eta_{al}\left(\left(\eta_{is,t}\dot{W}_{TG}\right) - \left(\eta_{is,c}\dot{W}_c\right)\right) \quad (25)$$

3. Results and Discussions

3.1 Variation in monthly energy production

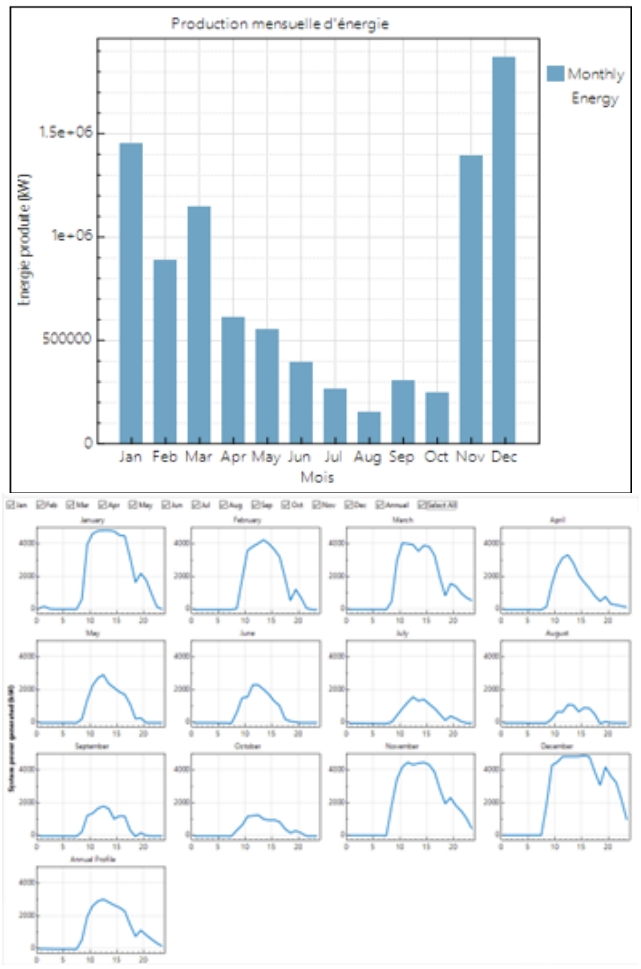

Figure 7: Average monthly energy production

Table: Annual production of electrical energy

Parameter	Value
Annual AC energy in year 1	7107210 kWh-e
Capacity factor	18.0%
Gross electrical power of the power cycle	7983170 kWh-e
kWh/kW at the first year	1579
Net Conversion	89.0 %
Annual water consumption	2394

It appears from these results that we have a maximum average monthly production in December and a minimum in August. This can be justified with the monthly average irradiation profile in the Ngaoundere area. The total annual energy produced is 7,107,210 kWh-e, with a capacity factor of 18% and a net conversion rate of 89%.

Also, thermal storage makes it possible to increase the quantity of total electrical energy produced during a day.

3.2 Incident thermal power and energy production

The electrical power of the plant is strongly linked to the thermal profile of the incident irradiation. The average number of hours of sunshine does not vary too much from one month to another. Thanks to thermal storage, a quantity of electrical energy is produced at night between 6 p.m. and 12 a.m. local time.

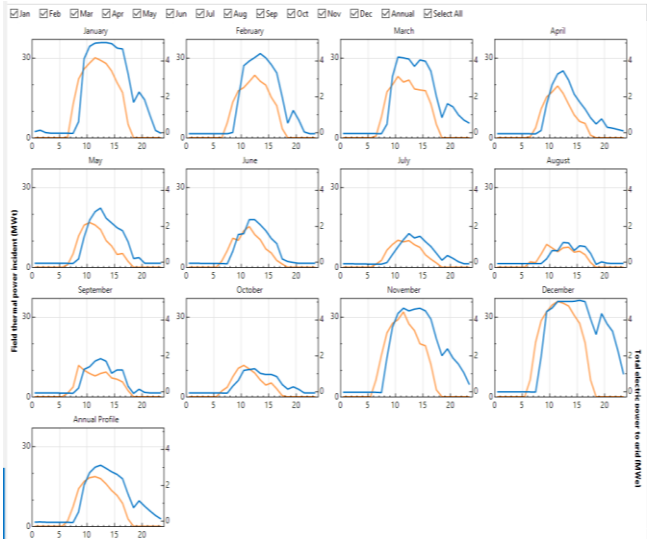

Figure 8: Incident thermal power and energy production

We have a peak electrical power of 5MWe for a peak incident thermal power of 35MWt observed in December.

3.3 Collector inlet and outlet temperatures

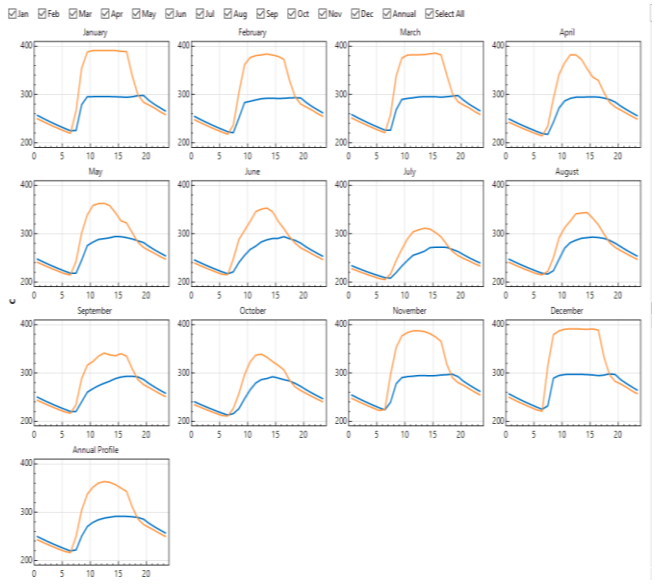

Figure 9: Collector inlet and outlet temperatures

In December and January, we have the best fluid temperature differences between the inlet (300°C) and outlet (400°C) of the collectors. In July and August, these temperature differences are the lowest, i.e. 35°C in July and 30°C in August.

3.4 Fluid mass flow and recirculation flow

Figure 10 below gives us the profile of the mass flow delivered by the solar field and the recirculation flow during the different months of the year for a day.

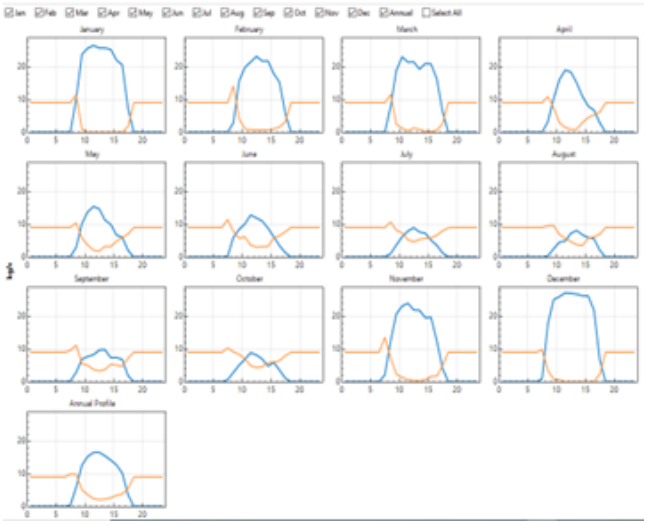

Figure 10: Delivered mass flow and recirculation mass flow

It appears from these curves that the maximum recirculation flow rate is 10 kg/s, while the maximum delivered mass flow rate is 27 kg/s and is obtained in the month of December.

4. Conclusion

Throughout this work, it was a question of contributing to the control of the energy parameters of a mini-mixed CSP/Biomass solar power plant with a view to providing a response to the energy problems of Northern Cameroon. It appears that the solar potential of the north is sufficient to operate a concentrated solar power plant, with an average irradiation of 5.12kWh/m^2/day. The hybrid power plant model studied consists of a concentrated solar electricity production system composed of a field of cylindrical-parabolic solar collectors, a recovery boiler, a steam turbine and a circulation pump operating according to a Rankine cycle, and a gas thermal electric production system composed of a compressor, a combustion chamber and a gas turbine operating according to a Brayton cycle. The gas used for combustion is bio-methane from the valorization of animal and plant biomass. The simulation was done only for the solar operating mode without hybridization. Electric power production varies from month to month. The electrical power is maximum in the months of December and January where it is around 5MWel and it is minimum in the months of August where it is around 1MWel. This power also varies from hour to hour during the day. It is zero outside of sunshine hours and is maximum between 12 p.m. and 2 p.m. The hybridization of the concentrated solar power plant with a gas power plant will make night-time production possible, but also stabilize the electrical power leaving the plant and regulate the additional production of the gas plant. Thermal storage allows the plant to operate for an additional 6 hours at night but at low speed. It also makes it possible to optimize the solar resource by increasing the quantity of energy produced daily compared to an identical system without thermal storage.

References

[1] Antoine AUROUUSSEAU, Dynamic modelling and regulation of linear thermodynamic solar power plants with direct steam generation, thesis - University of Toulouse, 2016.
[2] MINEPAT, National Development Strategy 2020-2030 P.43
[3] Brighter Africa: The growth potential of the sub-Saharan electricity sector (2015): https://www.mckinsey.com/~/media/McKinsey/dotcom/client_service/EPNG/PDFs/Brighter_ Africa-The_growth_potential_of_the_sub-Saharan_electricity_sector.ashx
[4] https://fr.climate-data.org , accessed June 1, 2022.
[5] NREL, NRSDB database.
[6] R. Kehlhofer, F. Hannemann, F. Stirnimann et al. “Combined-cycle gas and steam turbine power plants”. Third Edition, PennWell Corporation, Tulsa. 2009.
[7] R. Bhargava, M. Bianchi, A. De Pascale et al. “Gas turbine based power cycles - A state of the art Review”, Proceedings of the Power Engineering Conference, Hangzhou. 2007.
[8] A. Bölcs. “Thermal Turbomachines” Volume I, École Polytechnique Fédérale Lausanne.2001.
[9] Siemens Industrial Turbomachinery. “Industrial Gas Turbines: The Comprehensive Product Range from 5 to 50 Megawatts, Siemens AG”, Energy Sector, Erlangen. 2012.